# Behaviour of exponential three-point coordinates at the vertices of convex polygons

Dmitry Anisimov · Kai Hormann · Teseo Schneider

**Abstract**

Barycentric coordinates provide a convenient way to represent a point inside a triangle as a convex combination of the triangle's vertices and to linearly interpolate data given at these vertices. Due to their favourable properties, they are commonly applied in geometric modelling, finite element methods, computer graphics, and many other fields. In some of these applications, it is desirable to extend the concept of barycentric coordinates from triangles to polygons, and several variants of such generalized barycentric coordinates have been proposed in recent years. In this paper we focus on exponential three-point coordinates, a particular one-parameter family for convex polygons, which contains Wachspress, mean value, and discrete harmonic coordinates as special cases. We analyse the behaviour of these coordinates and show that the whole family is $C^0$ at the vertices of the polygon and $C^1$ for a wide parameter range.

**Citation Info**

*Journal*
Journal of Computational and Applied Mathematics

*Note*
Accepted

## 1 Introduction

Let $P$ be a strictly convex polygon with $n \geq 3$ vertices $v_1, \dots, v_n \in \mathbb{R}^2$ in anticlockwise order. We denote the interior of $P$ by the open set $\Omega \subset \mathbb{R}^2$ and its closure by $\bar{\Omega}$, so that $\bar{\Omega}$ is the convex hull of the vertices.

**Definition 1.** A set of functions $\lambda_1, \dots, \lambda_n \colon \bar{\Omega} \to \mathbb{R}$ is called a set of *generalized barycentric coordinates*, if the $\lambda_i$ satisfy the three properties

$$\text{1) Partition of unity:} \qquad \sum_{i=1}^{n} \lambda_i(v) = 1, \qquad v \in \bar{\Omega}, \tag{1a}$$

$$\text{2) Barycentric property:} \qquad \sum_{i=1}^{n} \lambda_i(v) v_i = v, \qquad v \in \bar{\Omega}, \tag{1b}$$

$$\text{3) Lagrange property:} \qquad \lambda_i(v_j) = \delta_{i,j}, \qquad i = 1, \dots, n, \quad j = 1, \dots, n, \tag{1c}$$

where $\delta_{i,j}$ is the Kronecker delta.

If $n = 3$, so that $P$ is a triangle, then it was already known to Möbius [5] that the corresponding barycentric coordinates are uniquely defined by

$$\lambda_i(v) = \frac{A(v, v_{i+1}, v_{i+2})}{A(v_1, v_2, v_3)}, \qquad i = 1, 2, 3,$$

where $A(x, y, z)$ denotes the signed area of the triangle $[x, y, z]$ with vertices $x, y, z \in \mathbb{R}^2$. Note that throughout this article we consider vertex indices cyclically over $1, \dots, n$, so that $v_{n+1} = v_1$ and $v_0 = v_n$, for example.

If $n \geq 4$, then such a unique definition does not exist, but Floater et al. [3] provide a simple recipe for constructing generalized barycentric coordinates. For any given set of functions $c_1, \dots, c_n \colon \Omega \to \mathbb{R}$, let

$$w_i(v) = \frac{c_{i+1}(v) A_{i-1}(v) - c_i(v) B_i(v) + c_{i-1}(v) A_i(v)}{A_{i-1}(v) A_i(v)}, \qquad i = 1, \dots, n, \tag{2}$$

where $A_i(v) = A(v, v_i, v_{i+1})$ and $B_i(v) = A(v, v_{i-1}, v_{i+1})$ are the signed triangle areas shown in Figure 1. The functions $\lambda_i \colon \Omega \to \mathbb{R}$ with

$$\lambda_i(v) = \frac{w_i(v)}{W(v)}, \qquad i = 1, \dots, n, \tag{3}$$

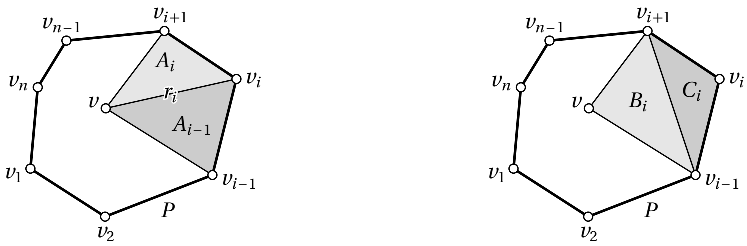


**Figure 1:** Notation used for the definition of exponential three-point coordinates for a planar polygon $P$ with vertices $v_1, \ldots, v_n$.

and

$$W(v) = \sum_{i=1}^{n} w_i(v), \tag{4}$$

are then well-defined and satisfy conditions (1a) and (1b) for any $v \in \Omega$, as long as the denominator $W(v)$ does not vanish. Moreover, if the $w_i$ in (2) are non-negative on $\Omega$, then the $\lambda_i$ extend continuously to $\bar{\Omega}$ and satisfy condition (1c). However, the non-negativity of the $w_i$ is only a sufficient condition and the recipe above usually leads to proper generalized barycentric coordinates even if it is not satisfied.

Floater et al. [3] further study the family of *exponential three-point coordinates*, which is defined by setting $c_i(v) = r_i(v)^p$ in (2) for some $p \in \mathbb{R}$ and $r_i(v) = \|v - v_i\|$ (see Figure 1). The name of this family refers to the exponent $p$ and the fact that $w_i(v)$ in (2) depends on the three vertices $v_{i-1}$, $v_i$, $v_{i+1}$ of $P$ for this choice of $c_i(v)$. They realize that Wachspress coordinates [7], mean value coordinates [2], and discrete harmonic coordinates [1, 6] are special members of this family for $p = 0$, $p = 1$, and $p = 2$, respectively, and that $p = 0$ and $p = 1$ are the only choices of $p$ for which the $w_i$ in (2) are positive. According to the sufficient condition mentioned above, this implies that Wachspress and mean value coordinates are generalized barycentric coordinates in the sense of Definition 1, but what about other values of $p$?

The plots in Figures 2 and 3 suggest that exponential three-point coordinates are well-defined over $\bar{\Omega}$ for other values of $p$, too, and in this paper we prove that they are proper generalized barycentric coordinates for any $p \in \mathbb{R}$. To this end, let us first observe that the denominator $W(v)$ in (4) does not vanish for any $v \in \Omega$.

**Proposition 1.** *Exponential three-point coordinates are well-defined over $\Omega$ for any $p \in \mathbb{R}$.*

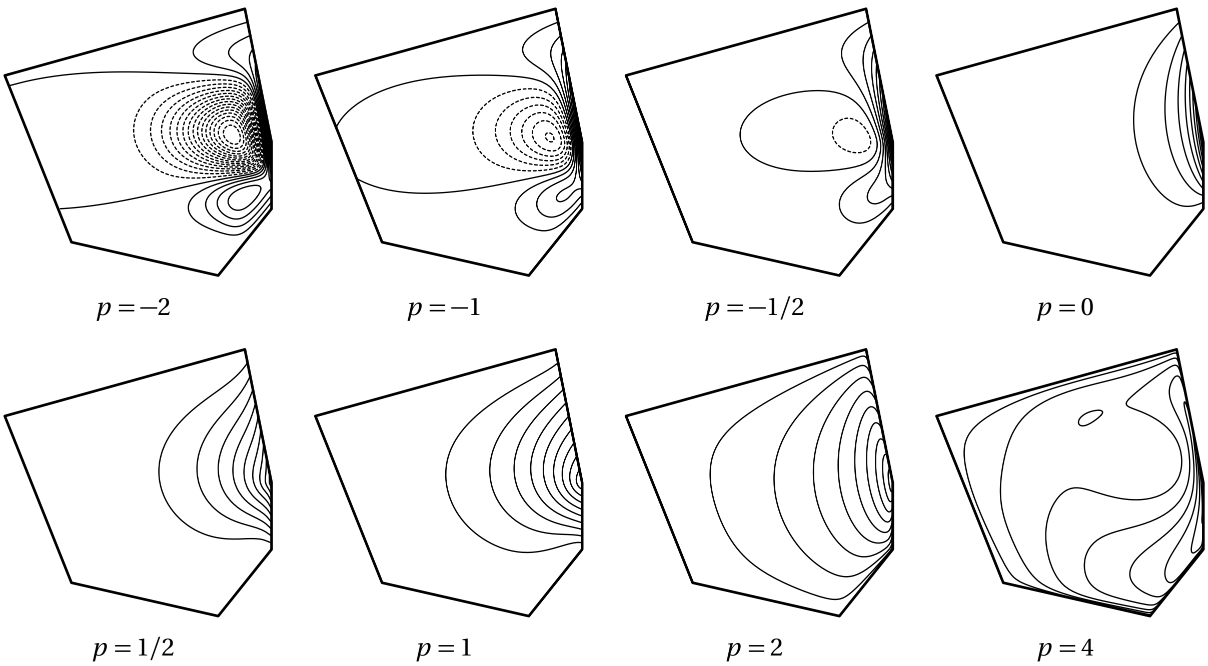


**Figure 2:** Contour plots for contour values $\mathbb{Z}/10$ of the exponential three-point coordinate corresponding to the middle right vertex of this convex polygon for different values of $p$. Dashed lines indicate negative contour values.

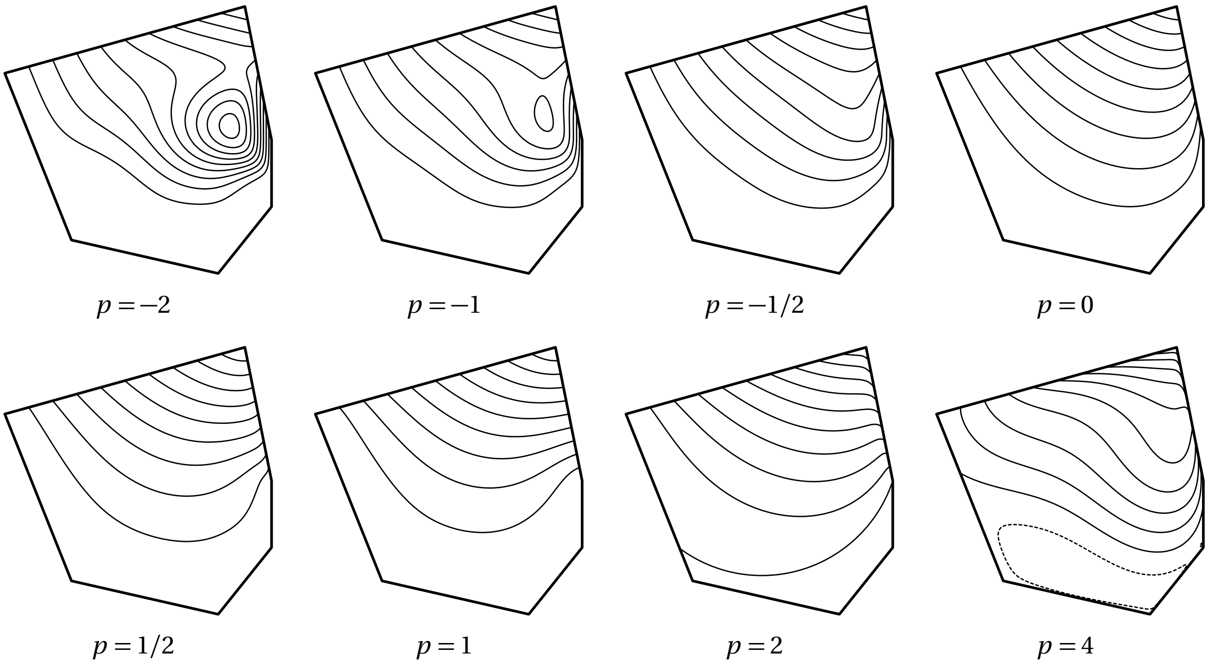


**Figure 3:** Contour plots for contour values $\mathbb{Z}/10$ of the exponential three-point coordinate corresponding to the top right vertex of this convex polygon for different values of $p$. Dashed lines indicate negative contour values.

*Proof.* Omitting the argument $v$ and noticing that $A_{i-1}+A_i = B_i + C_i$ with $C_i = A(v_{i-1}, v_i, v_{i+1})$, as shown in Figure 1, we can write $W$ as

$$
\begin{aligned}
W &= \sum_{i=1}^{n} \frac{r_{i+1}^p A_{i-1} - r_i^p (A_{i-1}+A_i - C_i) + r_{i-1}^p A_i}{A_{i-1}A_i} \\
&= \sum_{i=1}^{n} \frac{r_{i+1}^p - r_i^p}{A_i} + \sum_{i=1}^{n} \frac{r_i^p C_i}{A_{i-1}A_i} - \sum_{i=1}^{n} \frac{r_i^p - r_{i-1}^p}{A_{i-1}} \\
&= \sum_{i=1}^{n} \frac{r_i^p C_i}{A_{i-1}A_i},
\end{aligned}
\tag{5}
$$

which is clearly positive for $v \in \Omega$. Therefore, the $\lambda_i$ in (3) do not have any singularities in $\Omega$. □

Next, let us analyse the behaviour of the functions $\lambda_i$ as $v$ approaches any of the open edges $E_i = (v_i, v_{i+1})$, $i = 1,\dots,n$ of $P$. In this case, the area $A_i$ converges to zero, so that $w_i$ and $w_{i+1}$ diverge to infinity. We can fix this problem by introducing the products

$$
\mathcal{A} = \prod_{j=1}^{n} A_j, \qquad \mathcal{A}_i = \prod_{\substack{j=1\\ j\neq i}}^{n} A_j, \qquad \mathcal{A}_{i-1,i} = \prod_{\substack{j=1\\ j\neq i-1,i}}^{n} A_j, \qquad i=1,\dots,n,
$$

of all areas $A_j$ and those with one or two terms missing, respectively, and considering the functions

$$
\tilde{w}_i = w_i \mathcal{A} = r_{i+1}^p \mathcal{A}_i - r_i^p B_i \mathcal{A}_{i-1,i} + r_{i-1}^p \mathcal{A}_{i-1}, \qquad i=1,\dots,n, \tag{6}
$$

and

$$
\tilde{W} = W\mathcal{A} = \sum_{i=1}^{n} \tilde{w}_i. \tag{7}
$$

Since $\mathcal{A}$ is well-defined and does not vanish over $\Omega$, it is clear that the functions

$$
\tilde{\lambda}_i = \frac{\tilde{w}_i}{\tilde{W}}, \qquad i=1,\dots,n, \tag{8}
$$

coincide with the $\lambda_i$ on $\Omega$, but they have the advantage of being well-defined over the open edges of $P$.

**Proposition 2.** *Exponential three-point coordinates extend continuously to* $\Omega \cup E_1 \cup \cdots \cup E_n$ *and are linear along* $E_1, \ldots, E_n$ *for any* $p \in \mathbb{R}$.

*Proof.* Let us write $v \in E_j$ as $v = (1-t)v_j + t\,v_{j+1}$ for some $t \in (0,1)$ and note that $A_j(v) = 0$ and

$$-\frac{B_j(v)}{A_{j-1}(v)} = \frac{r_{j+1}(v)}{r_j(v)} = \frac{1-t}{t}.$$

Therefore, by (6) and omitting the argument $v$,

$$\tilde{w}_j = r_{j+1}^p \mathcal{A}_j + r_j^{p-1} r_{j+1} \mathcal{A}_j = \left(r_{j+1}^{p-1} + r_j^{p-1}\right) r_{j+1} \mathcal{A}_j$$

and similarly

$$\tilde{w}_{j+1} = \left(r_{j+1}^{p-1} + r_j^{p-1}\right) r_j \mathcal{A}_j.$$

Since $\tilde{w}_k = 0$ for $k \neq j, j+1$, we have

$$\tilde{W} = \tilde{w}_j + \tilde{w}_{j+1} = \left(r_{j+1}^{p-1} + r_j^{p-1}\right)\left(r_j + r_{j+1}\right)\mathcal{A}_j > 0$$

and conclude that the $\tilde{\lambda}_i$ are well-defined over $E_j$. Moreover,

$$\tilde{\lambda}_j = \frac{r_{j+1}}{r_j + r_{j+1}} = 1 - t, \qquad \tilde{\lambda}_{j+1} = \frac{r_j}{r_j + r_{j+1}} = t, \tag{9}$$

and $\tilde{\lambda}_k = 0$ for $k \neq j, j+1$. □

A similar trick can be used to show that the $\lambda_i$ also extend continuously to the vertices $v_j$ of $P$ and satisfy the Lagrange property (1c), but it requires a more refined and careful analysis (Section 2). We further investigate the behaviour of the derivatives of exponential three-point coordinates at the vertices and show that they are at least $C^1$ for any $p < 1$ (Section 3).

## 2 Continuity at the vertices

The functions $\tilde{\lambda}_i$ in (8) are not well-defined at the vertices of $P$, except for $p = 0$, but the linear behaviour along the edges $E_j$ in (9) implies that $\tilde{\lambda}_i(v)$ converges to $\delta_{i,j}$ as $v$ approaches $v_j$ along the boundary of $P$. It turns out that this behaviour also holds for $v$ approaching $v_j$ arbitrarily inside $P$ (Section 2.1), so that a continuous extension of exponential three-point coordinates to $\bar{\Omega}$ is obtained by enforcing the Lagrange property (1c). For $p \le 1$, the coordinates can further be extended to some region around $P$, but they have unremovable singularities arbitrarily close to the vertices for $p > 1$ (Section 2.2).

### 2.1 Convergence from inside

Let us first consider the case $p < 0$ and analyse the behaviour of the functions $\tilde{\lambda}_i$ as $v$ approaches some vertex $v_j$ of $P$. In this case, the distance $r_j$ converges to zero, so that $r_j^p$ and at least $\tilde{w}_j$ diverge to infinity. Similar to above, we can fix this problem by introducing the products

$$\mathcal{R} = \prod_{j=1}^{n} r_j^{-p}, \qquad \mathcal{R}_i = \prod_{\substack{j=1 \\ j \neq i}}^{n} r_j^{-p}, \qquad i = 1, \ldots, n,$$

and considering the functions

$$\hat{w}_i = \tilde{w}_i \mathcal{R} = \mathcal{R}_{i+1} \mathcal{A}_i - \mathcal{R}_i B_i \mathcal{A}_{i-1,i} + \mathcal{R}_{i-1} \mathcal{A}_{i-1}, \qquad i = 1, \ldots, n, \tag{10}$$

and

$$\hat{W} = \tilde{W} \mathcal{R} = \sum_{i=1}^{n} \hat{w}_i.$$

Since $\mathcal{R}$ is well-defined and does not vanish over $\Omega \cup E_1 \cup \cdots \cup E_n$, it is clear that the functions

$$\hat{\lambda}_i = \frac{\hat{w}_i}{\hat{W}}, \qquad i = 1, \ldots, n,$$

coincide with the $\tilde{\lambda}_i$ on $\Omega \cup E_1 \cup \cdots \cup E_n$, but they have the advantage of being well-defined at the vertices of $P$.

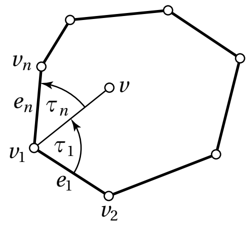


**Figure 4:** Notation used in the proofs of Lemmas 2 and 3.

**Lemma 1.** *Exponential three-point coordinates extend continuously to* $\bar{\Omega}$ *for* $p < 0$.

*Proof.* First observe that $A_{j-1}(v)$, $A_j(v)$, and $r_j(v)$ vanish at $v = v_j$. Therefore, $\mathcal{A}_i = 0$ for all $i$, $\mathcal{A}_{i-1,i} = \mathcal{R}_i = 0$ for $i \neq j$, and $\mathcal{A}_{j-1,j}, \mathcal{R}_j > 0$, so that all terms of the $\hat{w}_i$ in (10) vanish, except for the second term of $\hat{w}_j$. Consequently, $\hat{w}_i = 0$ for $i \neq j$, $\hat{w}_j = -\mathcal{R}_j B_j \mathcal{A}_{j-1,j} > 0$, $\hat{W} = \hat{w}_j > 0$, and finally $\hat{\lambda}_i(v_j) = \delta_{i,j}$. □

The reasoning in the proof of Lemma 1 does not carry over to the case $p > 0$, because $\mathcal{R}$ and $\mathcal{R}_i$ for $i \neq j$ diverge to infinity as $v$ approaches $v_j$. However, for $0 < p < 1$, this divergence is counterbalanced by the zero-convergence of the areas $A_{j-1}$ and $A_j$, so that the $\hat{w}_i$ converge to finite values at $v = v_j$.

**Lemma 2.** *Exponential three-point coordinates extend continuously to* $\bar{\Omega}$ *for* $0 < p < 1$.

*Proof.* Without loss of generality, we consider the case where $v$ approaches $v_1$, so that $A_1$, $A_n$, and $r_1$ converge to zero, while all other $A_i$ and $r_i$ converge to positive real numbers. The key idea now is to show that the two quotients $A_1/r_1^p$ and $A_n/r_1^p$ converge to zero, too. Denoting the length of $E_1$ by $e_1 = \|v_2 - v_1\|$ and the signed angle between the vectors $v_2 - v_1$ and $v - v_1$ by $\tau_1$ (see Figure 4), we can bound the first quotient as

$$0 \le \frac{A_1}{r_1^p} = \frac{r_1 e_1 \sin \tau_1}{2 r_1^p} \le \frac{r_1^{1-p} e_1}{2} \tag{11}$$

for any $v \in \Omega$. Since the upper bound is zero at $v = v_1$, we conclude

$$\lim_{v \to v_1} \frac{A_1(v)}{r_1(v)^p} = 0 \tag{12}$$

and similarly

$$\lim_{v \to v_1} \frac{A_n(v)}{r_1(v)^p} = 0. \tag{13}$$

It follows that all terms of the $\hat{w}_i$ in (10) with a diverging factor $\mathcal{R}_i$, $i \neq 1$, converge to zero, because they contain one of these two quotients. Among the other three terms with factor $\mathcal{R}_1$, which is finite at $v = v_1$, the terms in $\hat{w}_2$ and $\hat{w}_n$ are zero, because $\mathcal{A}_1$ and $\mathcal{A}_n$ vanish, so that only the second term in $\hat{w}_1$ is non-zero. Consequently, $\lim_{v \to v_1} \hat{w}_i(v) = 0$ for $i \neq 1$, $\lim_{v \to v_1} \hat{w}_1(v) = -\mathcal{R}_1(v_1) B_1(v_1) \mathcal{A}_{n,1}(v_1) > 0$, $\lim_{v \to v_1} \hat{W}(v) = \lim_{v \to v_1} \hat{w}_1(v)$, and therefore $\lim_{v \to v_1} \hat{\lambda}_i(v) = \delta_{i,1}$. □

The proof of Lemma 2 does not extend to the case $p > 1$, because the upper bound in (11) diverges. Going back to the functions $\tilde{\lambda}_i$ in (8), we see that they are not well-defined at the vertices of $P$, because all the $\tilde{w}_i$ and thus also $\tilde{W}$ are zero at $v = v_j$. However, for $p > 1$, this problem can be fixed by considering the functions $\tilde{w}_i / r_j$, $i = 1, \dots, n$, and $\tilde{W}/r_j$.

**Lemma 3.** *Exponential three-point coordinates extend continuously to* $\bar{\Omega}$ *for* $p > 1$.

*Proof.* As in the proof of Lemma 2, we consider only the case where $v$ approaches $v_1$. Like in (11), we can bound the quotients $A_1/r_1$ and $A_n/r_1$ for any $v \in \Omega$ as

$$0 \le \frac{A_1}{r_1} \le \frac{e_1}{2}, \qquad 0 \le \frac{A_n}{r_1} \le \frac{e_n}{2}, \tag{14}$$

where $e_n = \|v_n - v_1\|$ is the length of $E_n$ (see Figure 4). Since these bounds are constants, they also hold in the limit. For $i \neq 1$, we then observe that all terms of $\tilde{w}_i$ in (6) contain either $A_1$ or $A_n$ plus one other factor ($A_1$, $A_n$, $B_2$, $B_n$, or $r_1^p$) that vanishes at $v_1$, so that $\lim_{v \to v_1} \tilde{w}_i(v)/r_1(v) = 0$. It remains to show that

$$\frac{\tilde{w}_1}{r_1} = \left( \frac{r_2^p A_n}{r_1} - r_1^{p-1} B_1 + \frac{r_n^p A_1}{r_1} \right) \mathcal{A}_{n,1},$$

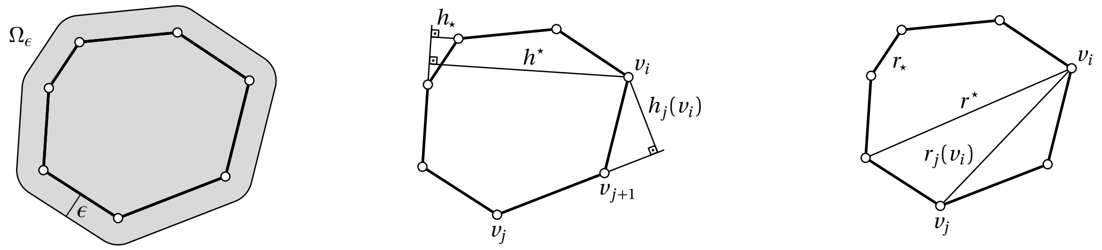


**Figure 5:** Notation used in Section 2.2.

and thus also $\tilde{W}/r_1$, converges to a non-zero, finite value. By (14),

$$\frac{r_2^p A_n}{r_1} + \frac{r_n^p A_1}{r_1} \le \frac{r_2^p e_n + r_n^p e_1}{2}$$

for any $v \in \Omega$ and this upper bound converges to the positive constant $c^\star = (e_1^p e_n + e_n^p e_1)/2$. Moreover,

$$\begin{aligned}\frac{r_2^p A_n}{r_1} + \frac{r_n^p A_1}{r_1} &= \frac{r_2^p e_n \sin\tau_n + r_n^p e_1 \sin\tau_1}{2}\\ &\ge \min(r_2, r_n)^p \min(e_1, e_n)(\sin\tau_1 + \sin\tau_n)/2\\ &\ge \min(r_2, r_n)^p \min(e_1, e_n)(\sin\tau_1 \cos\tau_n + \sin\tau_n \cos\tau_1)/2\\ &= \min(r_2, r_n)^p \min(e_1, e_n) \sin(\tau_1 + \tau_n)/2,\end{aligned}$$

where $\tau_n$ is the signed angle between $v - v_1$ and $v_n - v_1$ (see Figure 4), and this lower bound converges to the positive constant $c_\star = \min(e_1, e_n)^{p+1} \sin(\tau_1 + \tau_n)/2$. It follows that $(r_2^p A_n + r_n^p A_1)/r_1$ converges to a positive, finite value $c \in [c_\star, c^\star]$ and since $r_1^{p-1}$ vanishes at $v = v_1$ and $\mathcal{A}_{n,1}$ does not, the proof is complete. Note that the limit $c\mathcal{A}_{n-1}$ of $\tilde{w}_1/r_1$ may not be the same for two different sequences of $v$, which both converge to $v_1$, but this does not affect the proof, because the ratio $(\tilde{w}_1/r_1)/(\tilde{W}/r_1)$ always converges to 1. □

We are now ready to summarize our observations.

**Theorem 1.** *Exponential three-point coordinates are continuous generalized barycentric coordinates over $\bar{\Omega}$ for any $p \in \mathbb{R}$.*

*Proof.* It follows from Proposition 1 and Proposition 5 in [3] that exponential three-point coordinates are continuous and satisfy conditions (1a) and (1b) over $\Omega$ for any $p \in \mathbb{R}$. Proposition 2 and Lemmas 1, 2, and 3 further show that they can be extended continuously to $\bar{\Omega}$ for $p \notin \{0, 1\}$ and that this extension satisfies condition (1c) and is piecewise linear along the boundary of $P$. For $p = 0$ and $p = 1$, the same boundary behaviour follows from Corollary 2 in [3], and it implies that conditions (1a) and (1b) hold for any point on the boundary of $P$ and thus for any $v \in \bar{\Omega}$. □

## 2.2 Convergence from outside

Let us now enlarge the domain from $\bar{\Omega}$ to the open set $\Omega_\epsilon$ by adding all points $v \in \mathbb{R}^2$, which are $\epsilon$-close to $\Omega$ (see Figure 5), and analyse the continuity of exponential three-point coordinates over $\Omega_\epsilon$.

To this end, let $h_j(v)$ be the (shortest) distance between a point $v$ and the line through $v_j$ and $v_{j+1}$, and let

$$h_\star = \min_{\substack{i,j=1,\dots,n\\ j\ne i-1,i}} h_j(v_i), \qquad h^\star = \max_{i,j=1,\dots,n} h_j(v_i)$$

be the minimum and maximum distance between the vertices and the supporting lines of $P$. We further denote the minima and maxima of distances between vertices of $P$, of edge lengths, and of areas $C_i$ by

$$r_\star = \min_{\substack{i,j=1,\dots,n\\ j\ne i}} r_j(v_i), \qquad r^\star = \max_{i,j=1,\dots,n} r_j(v_i),$$

$$e_\star = \min_{i=1,\dots,n} \|v_i - v_{i+1}\|, \qquad e^\star = \max_{i=1,\dots,n} \|v_i - v_{i+1}\|,$$

$$C_\star = \min_{i=1,\dots,n} C_i, \qquad C^\star = \max_{i=1,\dots,n} C_i,$$

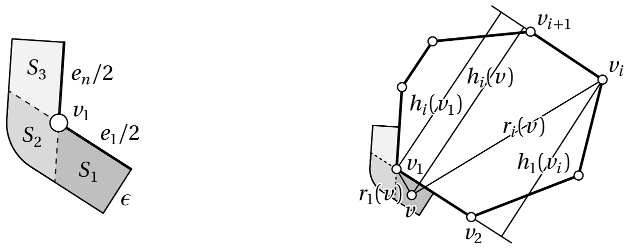


**Figure 6:** Notation used in the proofs of Lemmas 4 and 5.

respectively and finally introduce the positive constants

$$c_\star = \min(h_\star, r_\star, e_\star, C_\star), \qquad\qquad c^\star = \min(h^\star, r^\star, e^\star, C^\star), \tag{15}$$

which we use for defining upper bounds on $\epsilon$ that guarantee $\tilde{W}$ to be positive over $\Omega_\epsilon \setminus \bar{\Omega}$ for $p < 1$.

**Lemma 4.** *If* $p < 0$ *and*

$$\epsilon < \frac{c_\star}{n8^n}\left(\frac{c_\star}{c^\star}\right)^{2n-p}, \tag{16}$$

*then* $\tilde{W}(v) > 0$ *for any* $v \in \Omega_\epsilon \setminus \bar{\Omega}$.

*Proof.* Since $n \geq 3$, $p < 0$, and $c_\star \leq c^\star$, we conclude from (16) that

$$\epsilon < c_\star/4. \tag{17}$$

Without loss of generality, we now focus on the situation around $v_1$ and consider the three regions (see Figure 6)

$$\begin{aligned} S_1 &= \{v \in \Omega_\epsilon : A_1(v) < 0, A_n(v) \geq 0, r_1(v) \leq r_2(v)\}, \\ S_2 &= \{v \in \Omega_\epsilon : A_1(v) < 0, A_n(v) < 0\}, \\ S_3 &= \{v \in \Omega_\epsilon : A_1(v) \geq 0, A_n(v) < 0, r_1(v) \leq r_n(v)\}, \end{aligned} \tag{18}$$

because all other cases follow by symmetry.

Let us start with the case $v \in S_1$ and establish some bounds for $r_i(v)$ and $A_i(v)$. Since $v$ is closer to $v_1$ than to $v_2$, we can use the triangle inequality and (17) to get

$$r_1(v) \leq e_1/2 + \epsilon < e^\star/2 + c_\star/4 < c^\star$$

and thus

$$r_1^p > (c^\star)^p, \tag{19}$$

because $p < 0$. Moreover, since $v$ and $v_i$ for $i \geq 3$ lie on opposite sides of the line through $v_1$ and $v_2$, we have

$$r_i(v) > h_1(v_i) \geq h_\star \geq c_\star, \qquad i = 3, \ldots, n. \tag{20}$$

We next derive some bounds for $h_i(v)$, which then turn into bounds for $A_i(v)$ because $|A_i(v)| = e_i h_i(v)/2$. We first note that $h_1(v) < \epsilon$, hence

$$|A_1(v)| = e_1 h_1(v)/2 < e^\star \epsilon \leq c^\star \epsilon. \tag{21}$$

In general, we can get an upper bound for all $h_i(v)$ by triangle inequality,

$$h_i(v) \leq h_i(v_1) + r_1(v) < h^\star + c^\star \leq 2c^\star.$$

For $i = 2$, a lower bound can be obtained by recalling that $v$ is closer to $v_1$ than to $v_2$, so that

$$h_2(v) > h_2(v_1)/2 - \epsilon > h_\star/2 - c_\star/4 \geq c_\star/4.$$

For $i \geq 3$, the minimum distance from any point on the edge $[v_1, v_2]$ to the line through $v_i$ and $v_{i+1}$ is either $h_i(v_1)$ or $h_i(v_2)$, and so, since $v$ is $\epsilon$-close to $[v_1, v_2]$,

$$h_i(v) > \min(h_i(v_1), h_i(v_2)) - \epsilon > h_\star - c_\star/4 > c_\star/4.$$

Overall, we conclude that

$$\frac{(c_\star)^2}{8} < A_i(v) < (c^\star)^2, \qquad i = 2, \dots, n. \tag{22}$$

The idea now is to use (5) to rewrite $\tilde{W}$ in (7) as

$$\tilde{W} = r_1^p C_1 \mathcal{A}_{n,1} + r_2^p C_2 \mathcal{A}_{1,2} - |A_1| \sum_{i=3}^{n} r_i^p C_i \mathcal{A}_{1,i-1,i} \tag{23}$$

with

$$\mathcal{A}_{1,i-1,i} = \prod_{\substack{j=2 \\ j \neq i-1,i}}^{n} A_j, \qquad i = 3, \dots, n,$$

and to show that the first term in (23) dominates the last term. To this end, we observe that

$$\begin{aligned}
\frac{(c^\star)^p C_1 \mathcal{A}_{n,1}}{c^\star \sum_{i=3}^n r_i^p C_i \mathcal{A}_{1,i-1,i}} &\overset{(15)}{\geq} \frac{(c^\star)^p c_\star \mathcal{A}_{n,1}}{c^\star \sum_{i=3}^n r_i^p c^\star \mathcal{A}_{1,i-1,i}} \\
&\overset{(20)}{>} \frac{(c^\star)^p c_\star \mathcal{A}_{n,1}}{c^\star \sum_{i=3}^n (c_\star)^p c^\star \mathcal{A}_{1,i-1,i}} \\
&\overset{(22)}{>} \frac{(c^\star)^p c_\star (c_\star)^{2(n-2)}/8^{n-2}}{c^\star \sum_{i=3}^n (c_\star)^p c^\star (c^\star)^{2(n-3)}} = \frac{(c_\star)^{2n-3-p}}{(n-2)8^{n-2}(c^\star)^{2n-4-p}} \\
&\overset{(16)}{>} 2\epsilon,
\end{aligned}$$

where we obtain the second inequality by recalling that $p < 0$, and so

$$\frac{1}{2}(c^\star)^p C_1 \mathcal{A}_{n,1} > c^\star \epsilon \sum_{i=3}^{n} r_i^p C_i \mathcal{A}_{1,i-1,i}.$$

Using (19) and (21), we then conclude

$$\frac{1}{2} r_1^p C_1 \mathcal{A}_{n,1} > |A_1| \sum_{i=3}^{n} r_i^p C_i \mathcal{A}_{1,i-1,i}, \tag{24}$$

which implies $\tilde{W} > 0$, and similar arguments lead to

$$\frac{1}{2} r_1^p C_1 \mathcal{A}_{n,1} > |A_n| \sum_{i=2}^{n-1} r_i^p C_i \mathcal{A}_{n,i-1,i} \tag{25}$$

for the case $v \in S_3$.

If $v \in S_2$, then we rewrite $\tilde{W}$ as

$$\tilde{W} = r_1^p C_1 \mathcal{A}_{n,1} - |A_1| r_n^p C_n \mathcal{A}_{1,n-1,n} - |A_n| r_2^p C_2 \mathcal{A}_{n,1,2} + \sum_{i=3}^{n-1} r_i^p C_i \mathcal{A}_{i-1,i},$$

which is positive because of (24) and (25), which are also valid in this case. □

**Lemma 5.** *If* $0 \leq p < 1$ *and*

$$\epsilon < c_\star \left( \frac{1}{n 8^n} \left( \frac{c_\star}{c^\star} \right)^{2n} \right)^{\frac{1}{1-p}}, \tag{26}$$

*then* $\tilde{W}(v) > 0$ *for any* $v \in \Omega_\epsilon \setminus \bar{\Omega}$.

*Proof.* As in the proof of Lemma 4, it follows from (26) that $\epsilon < c_\star/4$, and we proceed by considering the first of the three regions in (18). For any $v \in S_1$, the bounds in (21) and (22) still hold, and we further observe that

$$|A_1(v)| = e_1 h_1(v)/2 \leq e^\star r_1(v)/2 < c^\star r_1(v)$$

and therefore

$$r_1^p \geq (|A_1|/c^\star)^p. \tag{27}$$

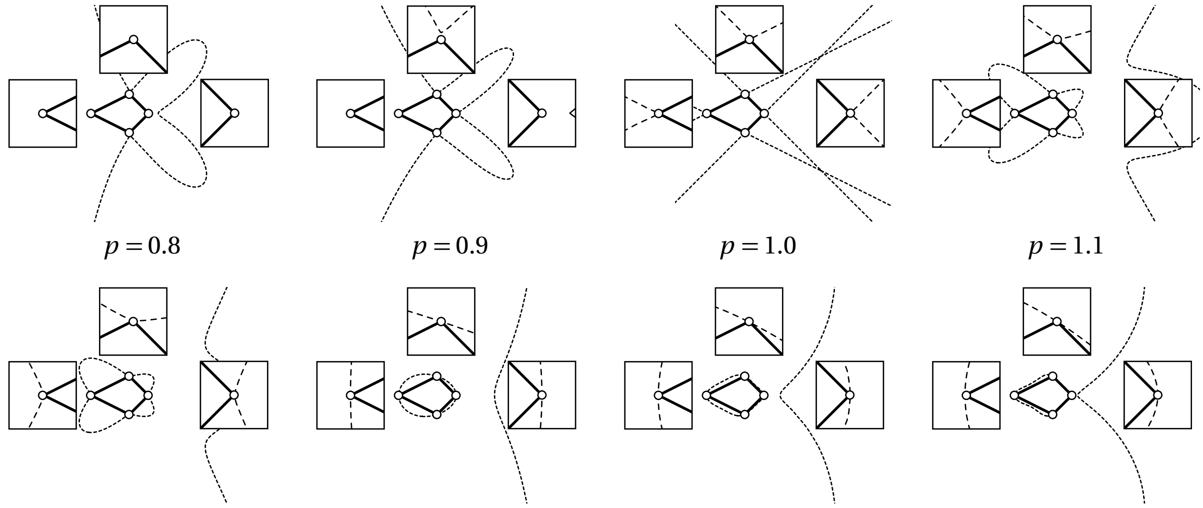

$p=0.8$ $p=0.9$ $p=1.0$ $p=1.1$

$p=1.2$ $p=2.0$ $p=3.0$ $p=4.0$

**Figure 7:** Plots of the zero level curve $\{v \in \mathbb{R}^2 : \tilde{W}(v)=0\}$ for a convex polygon with four vertices and different values of $p$. The close-ups to the vertices of the polygon use a magnification factor of 30.

Moreover, by triangle inequality we get the upper bound

$$r_i(v) \le r_1(v) + r_i(v_1) < e_1/2 + \epsilon + r_i(v_1) < c^\star/2 + c^\star/4 + c^\star < 2c^\star \tag{28}$$

for any $i$. With these bounds at hand we conclude that

$$\begin{aligned}
\frac{C_1 \mathcal{A}_{n,1}}{(c^\star)^p \sum_{i=3}^n r_i^p C_i \mathcal{A}_{1,i-1,i}} &\overset{(15)}{\ge} \frac{c_\star \mathcal{A}_{n,1}}{(c^\star)^p \sum_{i=3}^n r_i^p c^\star \mathcal{A}_{1,i-1,i}} \\
&\overset{(28)}{\ge} \frac{c_\star \mathcal{A}_{n,1}}{(c^\star)^p \sum_{i=3}^n (2c^\star)^p c^\star \mathcal{A}_{1,i-1,i}} \\
&\overset{(22)}{>} \frac{c_\star (c_\star)^{2(n-2)}/8^{n-2}}{(c^\star)^p \sum_{i=3}^n (2c^\star)^p c^\star (c^\star)^{2(n-3)}} = \frac{(c^\star)^{2(1-p)}}{2^p(n-2)8^{n-2}} \left(\frac{c_\star}{c^\star}\right)^{2n-3} \\
&> 2(c^\star)^{1-p}(c_\star)^{1-p} \frac{1}{n8^n} \left(\frac{c_\star}{c^\star}\right)^{2n} \\
&\overset{(26)}{>} 2(c^\star \epsilon)^{1-p} \\
&\overset{(21)}{>} 2|A_1|^{1-p},
\end{aligned}$$

so that

$$\frac{1}{2}(|A_1|/c^\star)^p C_1 \mathcal{A}_{n,1} > |A_1| \sum_{i=3}^n r_i^p C_i \mathcal{A}_{1,i-1,i}.$$

Using (27), we then get

$$\frac{1}{2} r_1^p C_1 \mathcal{A}_{n,1} > |A_1| \sum_{i=3}^n r_i^p C_i \mathcal{A}_{1,i-1,i},$$

which implies $\tilde{W} > 0$, exactly as in the proof of Lemma 4, and also the other cases $v \in S_3$ and $v \in S_2$ follow analogously. $\square$

The reasoning in Lemma 5 does not extend to the case $p=1$, because the upper bound in (26) converges to 0 as $p$ approaches 1. This suggests that $\tilde{W}$ vanishes at the vertices of $P$ for $p \ge 1$, and Figure 7 confirms that the zero level curve $\{v \in \mathbb{R}^2 : \tilde{W}(v)=0\}$ passes through the vertices of $P$ for $p \ge 1$. For $p=1$, this is not a problem, and Hormann and Floater [4] prove that the corresponding mean value coordinates are continuous over $\mathbb{R}^2$. But the following two examples show that exponential three-point coordinates for $p>1$ can have non-removable singularities in $\mathbb{R}^2 \setminus \bar{\Omega}$ arbitrarily close to the vertices of $P$, and so they are, in general, not continuous over $\Omega_\epsilon$ for any $\epsilon > 0$. Note that the polygons in both examples were chosen to keep

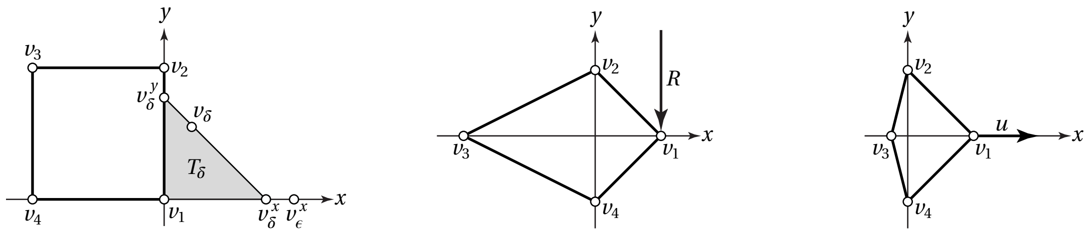


**Figure 8:** Notation used in Examples 1, 2, and 3.

the calculations as simple as possible, but we observed the same phenomena for all other polygons that we tested.

**Example 1.** Let us examine the exponential three-point coordinates for $1 < p < 2$ over the unit square $P$ with vertices $v_1 = (0,0)$, $v_2 = (0,1)$, $v_3 = (-1,1)$, $v_4 = (-1,0)$ (see Figure 8, left). For $x \geq 0$, it turns out that

$$\tilde{W}(x,0) = (x^p(1+x) - (1+x)^p x)/8,$$

hence $\tilde{W}(0,0) = 0$ and $(\partial \tilde{W}/\partial x)(0,0) = -1/8$, because $p > 1$. Consequently, there exists some $\epsilon \in (0,1)$, such that $\tilde{W}$ is negative over the open edge between $v_1 = (0,0)$ and $v_\epsilon^x = (\epsilon, 0)$, and from Proposition 2 we know that $\tilde{W}$ is positive over the open edge between $v_1$ and $v_\epsilon^y = (0,\epsilon)$. It follows that for any $\delta \in (0,\epsilon)$ there exists some point $v_\delta$ on the open edge $(v_\delta^x, v_\delta^y)$, such that $\tilde{W}(v_\delta) = 0$.

At least for the coordinate function $\lambda_3 = \tilde{w}_3/\tilde{W}$ it is easy to see that these singularities are non-removable close to $v_1$, because $\tilde{w}_3$ is negative over the open triangle $T_\delta = (v_1, v_\delta^x, v_\delta^y)$ for $\delta$ sufficiently small. To see this, we recall from (6) that $\tilde{w}_3 = \bar{w}_3 A_1 A_4$ with

$$\bar{w}_3(v) = r_4(v)^p A_2(v) - r_3(v)^p B_3(v) + r_2(v)^p A_3(v).$$

Since $\bar{w}_3(v_1) = 1 - 2^{\frac{p}{2}-1} > 0$ for $p < 2$, there exists some $\delta > 0$ such that $\bar{w}_3$ is positive over $T_\delta$. Therefore, $\tilde{w}_3$ is negative over $T_\delta$, because $A_1$ is negative and $A_4$ is positive over this region.

Despite the existence of these non-removable singularities, it seems hard to find an example of a sequence $(u_k)_{k\in\mathbb{N}}$ with $\lim_{k\to\infty} u_k = v_j$, such that $\lim_{k\to\infty} \lambda_i(u_k) \neq \lambda_i(v_j)$ in the case $1 < p < 2$. In particular, our numerical experiments suggest that $\lambda_i$ always converges to the correct value at $v_j$, if $v_j$ is approached along any line through $v_j$. This is not the case for $p \geq 2$, though.

**Example 2.** For the case $p \geq 2$, we consider the quadrilateral $P$ with vertices $v_1 = (1,0)$, $v_2 = (0,1)$, $v_3 = (-2,0)$, $v_4 = (0,-1)$ and study the behaviour of $\lambda_1$ along the vertical ray $R = \{(1,y) : y > 0\}$ (see Figure 8, middle). For $p = 2$, we find that $\lambda_1(1,y) = (9-4y^2)/15$ for $y > 0$, hence

$$\lim_{\substack{v\to v_1\\ v\in R}} \lambda_1(v) = \lim_{y\to 0^+} \lambda_1(1,y) = 3/5 < 1 = \lambda_1(v_1),$$

which shows that $\lambda_1$ is not continuous over $\Omega_\epsilon$ for any $\epsilon > 0$. For $p > 2$, we get

$$w_1(1,y) = 2\frac{(1+(1+y)^2)^{\frac{p}{2}} - (1+(1-y)^2)^{\frac{p}{2}}}{y} - 4y^{p-2}$$

for $y > 0$, and using L'Hôpital's rule, we obtain

$$\lim_{y\to 0^+} w_1(1,y) = 2^{\frac{p}{2}+1} p.$$

Similar reasoning shows that

$$\lim_{y\to 0^+} W(1,y) = 2^{\frac{p}{2}+1} p + 8(3^{p-1} - 2^{\frac{p}{2}})/3,$$

hence

$$\lim_{\substack{v\to v_1\\ v\in R}} \lambda_1(v) = \lim_{y\to 0^+} \frac{w_1(1,y)}{W(1,y)} = \frac{9p}{9p + 3^p 2^{2-\frac{p}{2}} - 12} < 1 = \lambda_1(v_1),$$

which again demonstrates that $\lambda_1$ is not continuous over $\Omega_\epsilon$ for any $\epsilon > 0$.

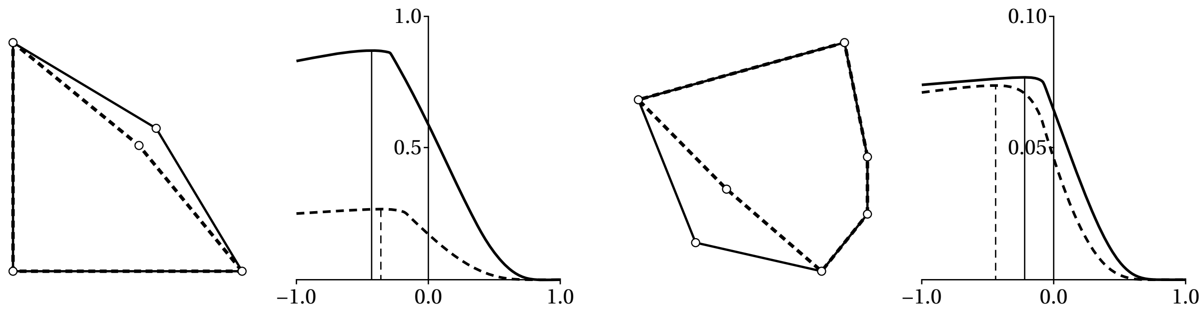


**Figure 9:** Plots of maximal $\epsilon$ over $p \in [-1,1)$, such that the exponential three-point coordinates are well-defined over the enlarged region $\Omega_\epsilon$ for four different convex polygons (solid and dashed lines) with common bounding box $[-1,1]^2$. The vertical lines in the plots indicate the values of $p$ that correspond to the largest maximal $\epsilon$ and hence allow for the biggest enlargement of $\Omega$.

We should point out that the direction of the ray $R$ does not by chance happen to be tangent to the zero level curve $\{v \in \mathbb{R}^2 : \tilde{W}(v) = 0\}$ at $v_1$ in this example. In fact, our numerical experiments suggest that $\lambda_i$ converges to the correct value at $v_j$ along any other line through $v_j$.

Let us conclude this section by summarizing our observations.

**Theorem 2.** *For any $p \leq 1$, there exists an $\epsilon > 0$, such that the exponential three-point coordinates are continuous generalized barycentric coordinates over $\Omega_\epsilon$.*

*Proof.* For $p = 1$, the statement is proven in [4], and for $p < 1$, it follows from Theorem 1, Lemmas 4 and 5, and by noting that Lemmas 1 and 2 carry over from $\bar{\Omega}$ to $\Omega_\epsilon$. The proof of Lemma 1 extends because $\hat{W}(v) > 0$ for any $v \in \Omega_\epsilon$, and the only change in the proof of Lemma 2 is that the lower bound for the quotient $A_1/r_1^p$ in (11) must be replaced by $-r_1^{1-p} e_1/2$, because $A_1$ can now be negative, but this does not affect the limit in (12) and similarly for the limit in (13). □

While the upper bounds on $\epsilon$ in Lemmas 4 and 5 are very small and of theoretical interest only, exponential three-point coordinates are well-defined over $\Omega_\epsilon$ for much larger values of $\epsilon$ in practice. Figure 9 reports the numerically determined maximal values of $\epsilon$ for some examples and $-1 \leq p < 1$. For the first polygon with vertices $v_1 = (-1,-1)$, $v_2 = (1,-1)$, $v_3 = (1/4, 1/4)$, $v_4 = (-1,1)$, the domain $\Omega$ can be enlarged by about half the shortest edge length, as long as $p$ is negative, with the maximum value of $\epsilon \approx 0.87$ occurring at $p \approx -0.43$. For positive $p$, the maximal $\epsilon$ decreases monotonically to values below 0.01 for $p \geq 0.72$. Replacing $v_3$ with $v_3 = (1/10, 1/10)$, as indicated by the dashed lines, does not change this behaviour, but scales the values by about 1/3, and they converge to 0 for all $p < 1$, as the exterior angle at $v_3$ converges to zero. The small exterior angle at the middle right vertex of the second polygon with six vertices (cf. Figures 2 and 3) is also the reason why the values of the maximal $\epsilon$ are smaller in this example, but the overall shape of the plot is similar, with the maximal value of $\epsilon \approx 0.077$ occurring at $p \approx -0.22$. Note how the position of the maximum changes as the exterior angle of the bottom left vertex becomes the dominating smallest exterior angle.

## 3 Differentiability at the vertices

Since exponential three-point coordinates are continuous over $\Omega_\epsilon$, and in particular in an $\epsilon$-neighbourhood of the vertices $v_j$ for $p \leq 1$, it seems natural to further study the differentiability at $v_j$. Wachspress coordinates ($p = 0$) are rational functions and therefore infinitely differentiable over $\Omega_\epsilon$ and in particular at $v_j$. Mean value coordinates ($p = 1$) instead have been shown [4] to be $C^\infty$ for any $v \in \mathbb{R}^2$, except at the vertices $v_j$, where they are only $C^0$. However, it turns out that the case $p = 1$ is very special (Section 3.1) and that three-point coordinates are at least $C^1$ at $v_j$ for any $p < 1$.

To carry out this analysis, let us remember the notion of the directional derivative

$$\nabla_u \hat{\lambda}_i(v_j) = \lim_{h \to 0} \frac{\hat{\lambda}_i(v_j + hu) - \hat{\lambda}_i(v_j)}{h}$$

of $\hat{\lambda}_i$ at $v_j$ in direction $u \in \mathbb{R}^2$, and that a necessary condition for the differentiability of $\hat{\lambda}_i$ at $v_j$ is the existence of a gradient $\nabla\hat\lambda_i(v_j)$, which satisfies

$$\nabla_u\hat\lambda_i(v_j) = \nabla\hat\lambda_i(v_j)\cdot u. \tag{29}$$

Because of the linear behaviour of exponential three-point coordinates along the edges $P$, as shown in Proposition 2, it is clear that the directional derivative along the adjacent edges $E_{j-1}$ and $E_j$, that is, in the directions $u^- = v_{j-1} - v_j$ and $u^+ = v_{j+1} - v_j$, is

$$\nabla_{u^-}\hat\lambda_i(v_j) = \begin{cases} 1, & i = j-1, \\ -1, & i = j, \\ 0, & \text{otherwise}, \end{cases} \qquad \text{and} \qquad \nabla_{u^+}\hat\lambda_i(v_j) = \begin{cases} -1, & i = j, \\ 1, & i = j+1, \\ 0, & \text{otherwise}, \end{cases} \tag{30}$$

respectively. Some simple algebra then shows that the only choice of $\nabla\hat\lambda_i(v_j)$ that satisfies (29) for $u = u^+$ and $u = u^-$, is

$$\nabla\hat\lambda_i(v_j) = \frac{1}{C_j}\begin{cases} \nabla A_j, & i = j-1, \\ -\nabla B_j, & i = j, \\ \nabla A_{j-1}, & i = j+1, \\ 0, & \text{otherwise}, \end{cases} \tag{31}$$

and this choice is indeed the limit of $\nabla\hat\lambda_i(v)$ as $v$ approaches $v_j$.

**Lemma 6.** *If $p < 1$, then*

$$\lim_{v\to v_j} \nabla\hat\lambda_i(v) = \nabla\hat\lambda_i(v_j), \qquad i = 1,\dots,n, \quad j = 1,\dots,n,$$

*with $\nabla\hat\lambda_i(v_j)$ defined as in* (31).

*Proof.* Without loss of generality, we only consider the case $j = 1$, so that $A_1$, $A_n$, $B_2$, $B_n$, and $r_1$ converge to zero as $v$ approaches $v_1$, while $B_1$ converges to $-C_1$ and all other $A_i$, $B_i$, and $r_i$ converge to positive real numbers. We recall from the proof of Lemma 2 that the quotients $A_1/r_1^p$ and $A_n/r_1^p$ converge to zero and note that similar arguments can be used to show that

$$\lim_{v\to v_1} \frac{B_2(v)}{r_1(v)^p} = 0, \qquad \lim_{v\to v_1} \frac{B_n(v)}{r_1(v)^p} = 0. \tag{32}$$

We also remember from the proof of Lemma 3 that the quotients $A_1/r_1$ and $A_n/r_1$ are bounded for any $v \in \Omega_\epsilon$ and likewise for the quotients $B_2/r_1$ and $B_n/r_1$, so that

$$\lim_{v\to v_1} \frac{A_1(v)A_n(v)}{r_1(v)^{p+1}} = 0, \qquad \lim_{v\to v_1} \frac{B_2(v)A_n(v)}{r_1(v)^{p+1}} = 0, \qquad \lim_{v\to v_1} \frac{B_n(v)A_1(v)}{r_1(v)^{p+1}} = 0. \tag{33}$$

We now apply the product rule to the right hand side of (10) to get

$$\nabla\hat w_i = \mathcal{R}_{i+1}\nabla\mathcal{A}_i + \mathcal{A}_i\nabla\mathcal{R}_{i+1} - \mathcal{R}_i B_i \nabla\mathcal{A}_{i-1,i} - \mathcal{R}_i\mathcal{A}_{i-1,i}\nabla B_i - \mathcal{A}_{i-1,i}B_i\nabla\mathcal{R}_i + \mathcal{A}_{i-1}\nabla\mathcal{R}_{i-1} + \mathcal{R}_{i-1}\nabla\mathcal{A}_{i-1},$$

and further expand this sum using

$$\nabla\mathcal{A}_k = \sum_{\substack{l=1\\ l\neq k}}^{n} \mathcal{A}_{k,l}\nabla A_l, \qquad \nabla\mathcal{R}_k = -p\mathcal{R}_k \sum_{\substack{l=1\\ l\neq k}}^{n} \frac{s_l}{r_l},$$

where $s_l(v) = (v - v_l)/r_l(v)$ is the unit vector pointing from $v_l$ into the direction of $v$. A careful analysis then reveals that most of the terms converge to zero for $i \neq 1$, because they contain at least one factor ($A_1$, $A_n$, $B_2$, or $B_n$) that vanishes at $v_1$ or one of the quotients in (12), (13), (32), or (33) that converge to zero, while all other factors either converge to finite values or (in the case of $s_1$) are bounded as $v$ approaches $v_1$. The only terms that do not converge to zero emerge from $\mathcal{R}_1\nabla\mathcal{A}_1$ in the case $i = 2$ and from $\mathcal{R}_1\nabla\mathcal{A}_n$ in the case $i = n$, and overall we get

$$\lim_{v\to v_1} \nabla\hat w_i(v) = \begin{cases} \mathcal{R}_1(v_1)\mathcal{A}_{n,1}(v_1)\nabla A_n, & i = 2, \\ 0, & i = 3,\dots,n-1, \\ \mathcal{R}_1(v_1)\mathcal{A}_{n,1}(v_1)\nabla A_1, & i = n. \end{cases} \tag{34}$$

The remaining gradient $\nabla\hat{w}_1$ diverges at $v_1$, but it turns out that multiplying it with any of the $\hat{w}_i$, $i=2,\dots,n$, which converge to zero as $v$ approaches $v_1$, as shown in the proofs of Lemmas 1 and 2, is sufficient to counterbalance the divergence. Indeed, it follows, using the same arguments as above, that

$$\lim_{v\to v_1}\hat{w}_i(v)\nabla\hat{w}_1(v)=0,\qquad i=2,\dots,n. \tag{35}$$

By the chain rule, (34), (35), and the fact that $\hat{W}$ converges to $\mathcal{R}_1(v_1)C_1\mathcal{A}_{n,1}(v_1)$, we finally get

$$\lim_{v\to v_1}\nabla\hat{\lambda}_i(v)=\lim_{v\to v_1}\left(\frac{\nabla\hat{w}_i(v)}{\hat{W}(v)}-\frac{\hat{w}_i(v)\sum_{j=1}^n\nabla\hat{w}_j(v)}{\hat{W}(v)^2}\right)=\frac{1}{C_1}\begin{cases}\nabla A_n, & i=2,\\ 0, & i=3,\dots,n-1,\\ \nabla A_1, & i=n.\end{cases}$$

For $i=1$, we note that $\hat{\lambda}_1=1-\sum_{i=2}^n\hat{\lambda}_i$ and therefore

$$\lim_{v\to v_1}\nabla\hat{\lambda}_1(v)=-\lim_{v\to v_1}\sum_{i=2}^n\nabla\hat{\lambda}_i(v)=-\frac{\nabla A_n+\nabla A_1}{C_1}=\frac{-\nabla B_1}{C_1},$$

where the last step follows from the fact that $A_n+A_1=B_1+C_1$. □

**Theorem 3.** *For any $p<1$, there exists an $\epsilon>0$, such that the exponential three-point coordinates are continuously differentiable over $\Omega_\epsilon$.*

*Proof.* Theorem 2 guarantees the existence of an $\epsilon$ for any $p<1$, such that $\hat{\lambda}_i$ is well-defined and continuous over $\Omega_\epsilon$. It further follows from (10) that $\hat{\lambda}_i$ is infinitely differentiable over $\Omega_\epsilon\setminus\bigcup_{j=1}^n v_j$, because $A_i$, $B_i$, and $r_i^{-p}$ are infinitely differentiable over this domain. Since the derivative of $\hat{\lambda}_i$ extends continuously to the $v_j$ by Lemma 6, the differentiability at $v_j$ follows by the multivariate mean value theorem. □

**Remark 1.** It has not escaped our notice that this result is somewhat little surprising for $p<0$. Clearly, if $p<-k$ for some $k\in\mathbb{N}_0$, then $r_j^{-p}$ is $C^k$, and it follows from (10) that $\hat{\lambda}_i$, as a combination of these $C^k$ functions and the $C^\infty$ functions $A_j$ and $B_j$, is $C^k$ itself. Taking a closer look at (10), we further find that each $r_j^{-p}$ can be paired with one of the linear functions $A_{j-1}$, $A_j$, $B_{j-1}$, or $B_{j+1}$, which vanish at $v_j$. Since these pairs are $C^{k+1}$, then so is $\hat{\lambda}_i$. Moreover, if $p=-2k$ for some $k\in\mathbb{N}$, then $\hat{\lambda}_i$ is a rational function, just as in the case of Wachspress coordinates ($p=0$), and likewise $C^\infty$ over $\Omega_\epsilon$. However, the result is still quite remarkable for $0<p<1$, because both the numerator $\hat{w}_i$ and the denominator $\hat{W}$ are only $C^0$ at the vertices $v_j$ in this case.

Figure 10 shows a close-up to an exponential three-point coordinate function in the region $\pm 10^{-5}$ around the corresponding vertex. For $p\le 1/2$, the coordinate is visually identical to a linear function. As $p$ increases, the slope of the function decreases inside and increases outside the polygon, but it remains $C^1$, as long as $p<1$. For $p=1$, the shape of the function is completely different, with a local, non-differentiable maximum at the vertex.

The proof of Lemma 6, and hence also Theorem 3, does not extend to the case $p\ge 1$, because the quotients in (33) diverge, and the following example shows that exponential three-point coordinates for $p\ge 1$ are, in general, not $C^1$ at the vertices of the polygon. As before, the polygon in the example was chosen to keep the formulas simple, but we observed the same phenomena for all other polygons that we tested.

**Example 3.** Let us consider the quadrilateral $P$ with vertices $v_1=(1,0)$, $v_2=(0,1)$, $v_3=(-1/4,0)$, $v_4=(0,-1)$ and study the directional derivative of $\hat{\lambda}_3$ in direction $u=(1,0)$ at $v_1$ (see Figure 8, right). If $\hat{\lambda}_3$ were $C^1$ at $v_1$, then, according to (29) and (31), we would have $\nabla_u\hat{\lambda}_3(v_1)=0$. Instead, we get

$$\nabla_u\hat{\lambda}_3(v_1)=\lim_{h\to 0}\frac{\hat{\lambda}_3(1+h,0)}{h}=\frac{16\left(\frac{5\sqrt{2}}{8}\right)^p-20}{25}<0$$

for $p>1$, while for $p=1$ only the one-sided limits

$$\lim_{h\to 0^-}\frac{\hat{\lambda}_3(1+h,0)}{h}=\frac{8\sqrt{2}-12}{5}<0\qquad\text{and}\qquad\lim_{h\to 0^+}\frac{\hat{\lambda}_3(1+h,0)}{h}=-\frac{4}{5}<0$$

exist.

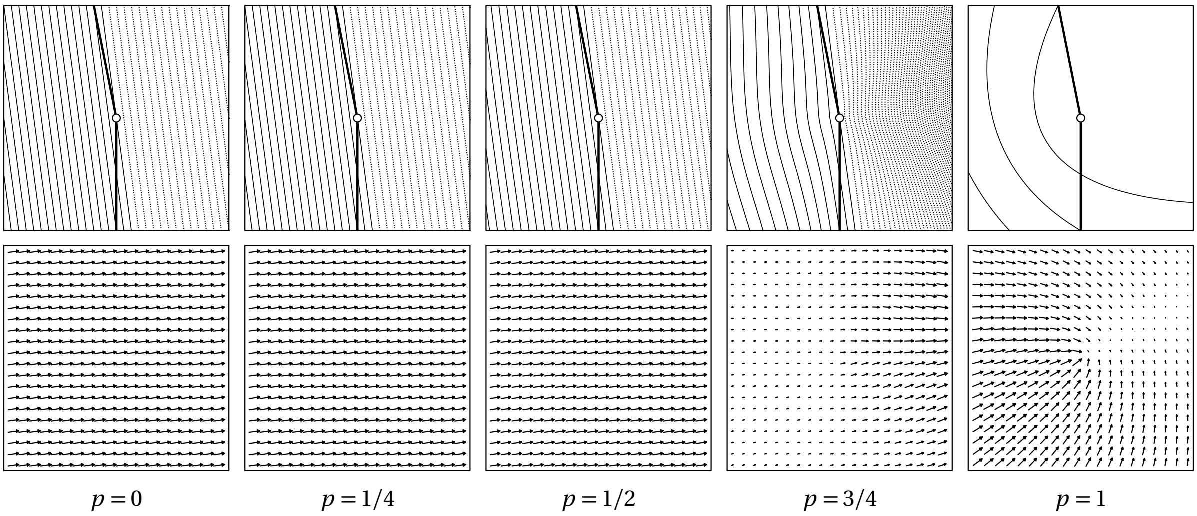


**Figure 10:** Contour plots (top) for contour values $\mathbb{Z}\cdot 10^{-5}$ and gradient vectors (bottom) of the exponential three-point coordinate corresponding to the middle right vertex of the convex polygon in Figure 9 (right) for different values of $p$ (cf. Figure 2). Dotted lines indicate contour values greater than one.

### 3.1 Directional derivatives of mean value coordinates

It is clear that the directional derivatives of a $C^1$ function $f\colon \mathbb{R}^2 \to \mathbb{R}$ at $v \in \mathbb{R}^2$ in the unit directions $u \in S^1$ form a sinusoidal function with period $2\pi$, because

$$\nabla_u f(v) = \nabla f(v)\cdot u = \|\nabla f(v)\| \cos\phi,$$

where $\phi$ is the angle between $\nabla f(v)$ and $u$. The plots in Figure 11 confirm that this is exactly how exponential three-point coordinates for $p<1$ behave at the vertices. Instead, for mean value coordinates ($p=1$), which are not $C^1$ at the vertices, the plots suggest that the one-sided directional derivatives also form a sinusoidal function with period $2\pi$, but with non-zero vertical shift in this case.

To prove this interesting observation, we recall the definition of the one-sided directional derivative

$$\nabla_u^+ \lambda_i(v_j) = \lim_{h\to 0^+} \frac{\lambda_i(v_j+hu)-\lambda_i(v_j)}{h}$$

of $\lambda_i$ at $v_j$ in direction $u\in\mathbb{R}^2$ and define the normals

$$n_i = \frac{2v_i - v_{i-1} - v_{i+1}}{\|2v_i - v_{i-1} - v_{i+1}\|}, \qquad i=1,\dots,n,$$

that bisect the exterior angles at $v_i$.

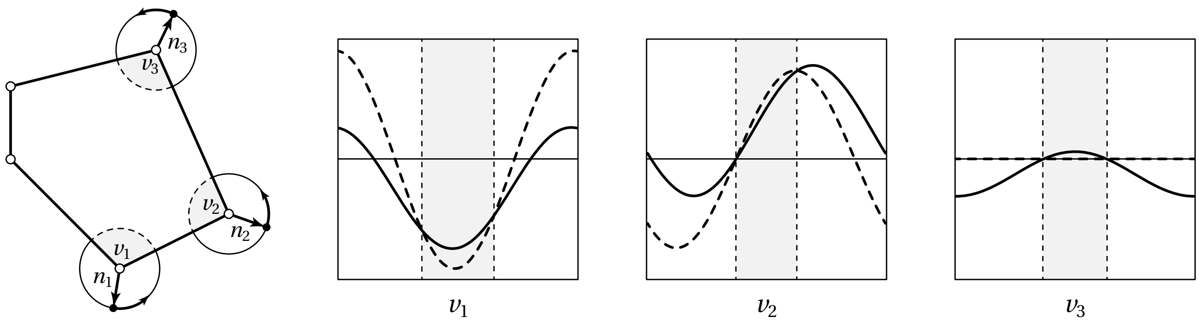


**Figure 11:** One-sided directional derivatives of $\lambda_1$ at $v_1$, $v_2$, and $v_3$ for $p<1$ (dashed) and $p=1$ (solid), parameterized by the signed angle to the normal $n_1$, $n_2$, and $n_3$, respectively. The grey area corresponds to the interval of the angle inside the polygon.

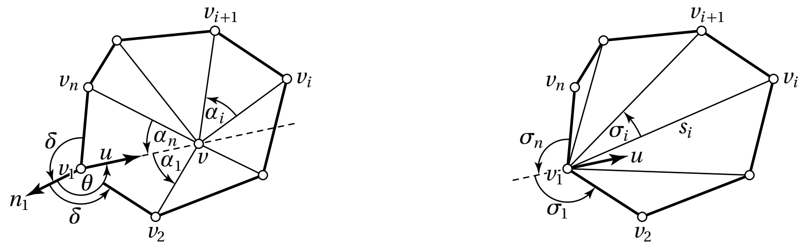


**Figure 12:** Notation used in the proof of Theorem 4.

**Theorem 4.** *The one-sided directional derivatives of mean value coordinates ($p=1$) at $v_j$ in the unit directions $u \in S^1$ can be written as*

$$\nabla_u^+ \lambda_i(v_j) = a_{i,j}(\sin(\theta+\varphi_{i,j}) + b_{i,j}), \qquad i=1,\dots,n, \quad j=1,\dots,n,$$

*where $\theta$ is the signed angle between $n_i$ and $u$, and $a_{i,j}$, $b_{i,j}$, $\varphi_{i,j}$ are certain constants depending on $P$.*

*Proof.* As shown in [3], mean value coordinates can also be defined by replacing the $w_i$ in (2) with

$$w_i = \frac{\tan(\alpha_{i-1}/2) + \tan(\alpha_i/2)}{r_i}, \qquad i=1,\dots,n$$

where $\alpha_i$ is the signed angle between $v_i - v$ and $v_{i+1} - v$ (see Figure 12). The advantage of this formula is that it can be used to evaluate the resulting coordinates $\lambda_i$ everywhere, except at the boundary of the polygon, because the denominator $W$ is non-zero for all $v \in \mathbb{R}^2 \setminus \partial\Omega$ [4].

Without loss of generality, we focus on the case $j=1$ and consider the situation as $v$ approaches $v_1$ along the ray defined by some unit vector $u \in S^1$ (see Figure 12). For the moment, we tacitly assume that $u$ is not pointing along the adjacent edges $E_1$ and $E_n$, so that $w_i(v_1+hu)$ is well-defined for sufficiently small $h>0$. Denoting the signed angle between $n_1$ and $u$ by $\theta$, it is clear that $\alpha_1$ and $\alpha_n$ converge to

$$\sigma_1 = \lim_{h\to 0^+} \alpha_1(v_1+hu) = \delta + \pi - \theta \qquad \text{and} \qquad \sigma_n = \lim_{h\to 0^+} \alpha_n(v_1+hu) = \delta + \theta - \pi,$$

where $\delta$ is the signed angle between $n_1$ and $v_2 - v_1$ and between $v_n - v$ and $n_1$ (see Figure 12). Letting $\sigma_i = \alpha_i(v_1)$, $i=2,\dots,n-1$ and $s_i = r_i(v_1)$, $i=2,\dots,n$, we have

$$\lim_{h\to 0^+} w_i(v_1+hu) = \frac{\tan(\sigma_{i-1}/2) + \tan(\sigma_i/2)}{s_i}, \qquad i=2,\dots,n.$$

Moreover, since $r_1(v_1+hu) = h$,

$$\lim_{h\to 0^+} h w_i(v_1+hu) = \begin{cases} \tan(\sigma_n/2) + \tan(\sigma_1/2), & i=1, \\ 0, & i=2,\dots,n. \end{cases}$$

For $i=3,\dots,n-1$, we then get

$$\begin{aligned} \nabla_u^+ \lambda_i(v_1) = \lim_{h\to 0^+} \frac{w_i(v_1+hu)}{hW(v_1+hu)} &= \frac{\tan(\sigma_{i-1}/2) + \tan(\sigma_i/2)}{s_i} \cdot \frac{\cos(\sigma_n/2)\cos(\sigma_1/2)}{\sin((\sigma_n+\sigma_1)/2)} \\ &= \frac{\tan(\sigma_{i-1}/2) + \tan(\sigma_i/2)}{2 s_i \sin\delta}\big(\sin(\theta - \pi/2) + \sin(\delta + \pi/2)\big), \end{aligned}$$

and similarly, after some trigonometric simplifications,

$$\nabla_u^+ \lambda_2(v_1) = \frac{1}{2 s_2 \sin\delta \cos(\sigma_2/2)}\big(\sin(\theta - \sigma_2/2) + \sin(\delta + \sigma_2/2)\big)$$

and

$$\nabla_u^+ \lambda_n(v_1) = \frac{-1}{2 s_n \sin\delta \cos(\sigma_{n-1}/2)}\big(\sin(\theta + \sigma_{n-1}/2) - \sin(\delta + \sigma_{n-1}/2)\big).$$

If $u$ is pointing along the adjacent edges $E_1$ or $E_n$, so that $\theta = \delta$ or $\theta = -\delta$, then these formulas give the correct values, and so they are valid for all $u \in S^1$. For the remaining case $i = 1$ we note that

$$\nabla_u^+ \lambda_1(v_1) = \lim_{h \to 0^+} \frac{w_1(v_1 + hu) - W(v_1 + hu)}{hW(v_1 + hu)} = \lim_{h \to 0^+} \sum_{i=2}^{n} \frac{-w_i(v_1 + hu)}{hW(v_1 + hu)} = -\sum_{i=2}^{n} \nabla_u^+ \lambda_i(v_1)$$

and that a sum of sinusoidal functions with period $2\pi$ is also a sinusoidal function with the same period. $\square$

An immediate consequence of Theorem 4 is that the one-sided directional derivatives of mean value coordinates at the vertices are bounded. Further note that Theorem 4 also holds in the case of non-convex polygons, because the convexity of $P$ is not used in the proof.

**Remark 2.** For $p > 1$, a similar analysis, based on the alternative representation of the coordinates $\lambda_i$ using

$$w_i = \frac{1}{r_i} \left( \frac{r_{i-1}^{p-1} - r_i^{p-1} \cos \alpha_{i-1}}{\sin \alpha_{i-1}} + \frac{r_{i+1}^{p-1} - r_i^{p-1} \cos \alpha_i}{\sin \alpha_i} \right), \qquad i = 1, \dots, n$$

instead of the $w_i$ in (2), reveals that the one-sided directional derivatives of $\lambda_i$ at $v_j$ in the unit directions $u \in S^1$ can be written as

$$\nabla_u^+ \lambda_i(v_j) = a_{i,j} \frac{\sin(2\theta + \varphi_{i,j}) + b_{i,j}}{\sin(\theta + \psi_j)}, \qquad i = 1, \dots, n, \quad j = 1, \dots, n,$$

for certain constants $a_{i,j}$, $b_{i,j}$, $\varphi_{i,j}$, $\psi_j$ depending on $P$. Note that the phase shift $\psi_j$ in the denominator does not depend on $i$, and it can be shown that the common poles of all one-sided directional derivatives $\nabla_u^+ \lambda_i(v_j)$, $i = 1, \dots, n$ at $v_j$ occur in the directions $u = \pm t / \|t\|$, where

$$t = \big( (v_{j+1} - v_j) \|v_{j-1} - v_j\|^p - (v_{j-1} - v_j) \|v_{j+1} - v_j\|^p \big),$$

and that $t$ is tangent to the zero level curve $\{v \in \mathbb{R}^2 : \tilde{W}(v) = 0\}$. As both these directions clearly lie outside $P$, the one-sided directional derivatives are well-defined and bounded over $\bar{\Omega}$.

## 4 Conclusion

Based on the results above, we can split the family of exponential three-point coordinates for planar convex polygons into three sub-families with different behaviour: (1) for $p < 1$, which includes Wachspress coordinates ($p = 0$), these coordinates are well-defined and at least $C^1$ in an $\epsilon$-neighbourhood of the polygon; (2) for $p > 1$, which includes discrete harmonic coordinates ($p = 2$), they are well-defined over the polygon, but not necessarily in its vicinity and only $C^0$ at the vertices of the polygon; (3) mean value coordinates ($p = 1$) are well-defined and $C^\infty$ everywhere in the plane, except at the vertices, where they are $C^0$ with bounded directional derivatives.


### Acknowledgements

We wish to thank Ulrich Reif for inspiring discussions and helpful comments. This work was supported by the Swiss National Science Foundation (SNSF) under project numbers 200020_156178 and P2TIP2_175859.


### References


[1] M. Eck, T. DeRose, T. Duchamp, H. Hoppe, M. Lounsbery, and W. Stuetzle. Multiresolution analysis of arbitrary meshes. In *Proceedings of SIGGRAPH*, pages 173–182, Los Angeles, Aug. 1995.

[2] M. S. Floater. Mean value coordinates. *Computer Aided Geometric Design*, 20(1):19–27, Mar. 2003.

[3] M. S. Floater, K. Hormann, and G. Kós. A general construction of barycentric coordinates over convex polygons. *Advances in Computational Mathematics*, 24(1–4):311–331, Jan. 2006.

[4] K. Hormann and M. S. Floater. Mean value coordinates for arbitrary planar polygons. *ACM Transactions on Graphics*, 25(4):1424–1441, Oct. 2006.

[5] A. F. Möbius. *Der barycentrische Calcul.* Johann Ambrosius Barth Verlag, Leipzig, 1827.

[6] U. Pinkall and K. Polthier. Computing discrete minimal surfaces and their conjugates. *Experimental Mathematics*, 2(1):15–36, 1993.

[7] E. L. Wachspress. *A Rational Finite Element Basis*, volume 114 of *Mathematics in Science and Engineering*. Academic Press, New York, 1975.